Available online at www.sciencedirect.com
SCIENCE DIRECT®
Coastal Engineering 52 (2005) 139–149
Coastal Engineering
An International Journal for Coastal, Harbour and Offshore Engineers
www.elsevier.com/locate/coastaleng

Improved parabolic water wave transformation model

U.M. Saied*, I.K. Tsanis

Department of Civil Engineering, McMaster University, 1280 Main Street West, ONT., Hamilton, Canada L8S 4L7

Received 4 September 2003; received in revised form 3 August 2004; accepted 1 October 2004
Available online 10 November 2004

Abstract

An improved parabolic water wave transformation model is developed based on generalized [1/1] Padé approximation. For forward scattered waves, the parabolic equation is solved using a marching scheme. The values of wave angles are calculated after the solution of each line; so that better [1/1] generalized Padé approximation is performed. The nonlinear effects are included using a modified dispersion equation. The model is easy to use and performs very well for complex bathymetry. The model is tested for cases of wave angles up to 70°. The numerical results show that for large wave angles, the new parabolic model is better than all the existing parabolic models based on rational approximation.

Keywords: Padé approximation; Mild slope equation; Parabolic wave model

1. Introduction

The combined refraction–diffraction wave equation, known as the mild slope equation, derived by Berkhoff (1972) has been widely used in coastal engineering. The mild slope equation can also model the wave reflections due beaches or coastal structures. It was derived under the assumption of mild bottom slope. However, Booij (1981) showed that this equation is satisfactory even for bottom slope of the order of unity.

The mild slope equation, being elliptic, is computationally demanding. Therefore, parabolic approximations are very useful in cases where wave reflections are not important. Several parabolic models have been proposed. The mild slope equation used to derive the parabolic equation is of the form of Helmholtz equation (Li, 1997):

$$\nabla^2\psi + k_c^2\psi = 0 \tag{1}$$

where $\psi=(cc_g)^{1/2}\Psi$, Ψ is the complex velocity potential, and k_c is the modified wave number, which is given by:

$$k_c^2 = k^2 - \frac{\nabla^2\left(cc_g\right)^{1/2}}{\left(cc_g\right)^{1/2}} \tag{2}$$

where c is the wave phase velocity, c_g is the wave group velocity, ω is the angular wave frequency and k

* Corresponding author.
E-mail address: saiedum@mcmaster.ca (U.M. Saied).

0378-3839/$ - see front matter © 2004 Elsevier B.V. All rights reserved.
doi:10.1016/j.coastaleng.2004.10.001

is the wave number, which is related to the wave angular frequency through the dispersion equation:

$$\omega^2 = gk\tanh(kd) \tag{3}$$

where, d is the local water depth and g is the gravitational acceleration.

Assuming that the water depth is constant, Eq. (1) can be written as:

$$A_{xx} + 2ikA_x + A_{yy} = 0 \tag{4}$$

where A is the amplitude function, which is given by:

$$\Psi = A\exp(ikx) \tag{5}$$

Assuming that x is the predominant direction of wave propagation.

Radder (1979) assumed that the derivatives of the wave potential in the x-direction are very small, which leads to:

$$2ikA_x + A_{yy} = 0 \tag{6}$$

Eq. (6) is considered the lowest-order parabolic approximation of the Helmholtz equation which corresponds to [1/0] Padé approximation or the lowest order binomial expansion.

A possible plane wave solution can be given by:

$$A = a\exp ik[(l-1)x + my] \tag{7}$$

where l=cos θ, m=sin θ, and θ is the wave angle measured counterclockwise from x-direction.

Substituting Eq. (7) into Eq. (4), the relationship between l and m can be found as follows:

$$l_h = \sqrt{1-m^2} \tag{8}$$

where l_h is cosine the wave angle according to Helmholtz equation. Eq. (8) represents a circle. However, substituting Eq. (7) into Eq. (6) leads to the following first order parabolic approximation:

$$l_a = 1 - \frac{1}{2}m^2 \tag{9}$$

where, l_a is the approximated cosine of the wave angle. Eq. (9) corresponds to the first order binomial expansion for the square root in Eq. (8). Radder's simple parabolic model (Eq. (9) or (6)) can accurately predict the propagation of plane waves with angles up to 43° without creating more than 5% error in l, where the error in l is defined as $(l_h - l_a)/l_h \times 100$ (Li, 1997).

Other parabolic approximations are obtained by approximating the square root in Eq. (8). Booij (1981) developed a higher order parabolic model, which permits waves angles up to 56.5°. For constant water depth, this parabolic model can be written as:

$$2ikA_x + A_{yy} + iA_{xyy}/2k = 0 \tag{10}$$

Substituting Eq. (7) into Eq. (10), it can be found that Booij's model is based on [1/1] Padé approximation of l.

Kirby (1986b) provided a [2/2] Padé approximation of l which leads to the following parabolic equation:

$$2ikA_x + A_{yy} - 3A_{xyy}/2ik - A_{xyyyy}/8ik^3 + A_{yyyy}/2k^2 = 0 \tag{11}$$

which is accurate up to 68°.

Kirby (1986b) utilized a minimax approach to approximate the square root in Eq. (8). For constant water depth, his parabolic model reads (Li, 1997):

$$2ikA_x + 2(b_1 - a_1)A_{yy} - 2ib_1A_{xyy}/k + 2k(a_0 - 1)A = 0 \tag{12}$$

where the values a_0, a_1, and b_1 are found by requiring that the error in l be minimized over a given range of wave angles. The approximated l can be found as follows:

$$l_a = \frac{a_0 + a_1m^2}{1 + b_1m^2} \tag{13}$$

The results of this equation at large wave angles are approximately as accurate as Eq. (11).

According to Li (1997), Dalrymple and Kirby (1988) developed a wide-angle model based on the Fourier transform method for a bathymetry consisting of parallel contours. Their analysis shows that the wave field can be decomposed into an angular

spectrum; that is the superposition of many synchronous wave trains propagating at different angles to the x-axis varying from 0° to ±90°. Dalrymple et al. (1989) extended this model to the irregular bathymetry situation. Although there is no longer an angle limitation for this model, the formulas are quite complicated, and the CPU time required is more than that for other parabolic models (Li, 1997).

Li (1997) developed a nonlinear parabolic approximation for the Helmholtz equation. His model does not have angle limitation for forward wave propagation.

In this paper, a new parabolic model is developed based on the generalized Padé approximation (Saied and Tsanis, 2004). The new model is tested for complex bathymetry using the experiment reported by Berkhoff (1982). The case of circular shoal over flat bottom reported by Kirby (1986b) is chosen to test the new model for large wave angles. The new parabolic model results are compared with Li's (1997) model and Kirby's (1986b) model.

2. Parabolic model

Kirby (1986b) developed a parabolic model for weakly nonlinear waves on slowly varying depth based on the approximation given by Eq. (13). The values of the coefficients a_0, a_1, and b_1 are evaluated by the minimax approach which minimizes the error in l over a given range of wave angles. He solved for the forward-scattered waves only, which has a possible plane wave solution on the form:

$$\Psi^{+} = A\exp\left(i\int \bar{k}(x)\mathrm{d}x\right) \tag{14}$$

where $\bar{k}(x)$ is some average of $k(x,y)$ over the y-direction and where the wave phase is assumed to accumulate principally in the x-direction.

Kirby and Dalrymple (1986) developed an approximate composite dispersion relation in order to model nonlinear effects over a broad range of depths, which reads:

$$\omega^2 = gk[1 + (ka)^2 F_1 D]\tanh[kd + (ka)F_2] \tag{15}$$

where a is the wave amplitude=$H/2$, H is the wave height and F_1, F_2 and D are functions given as follows:

$$D = \frac{\cosh(4kd) - 8 + 2\tanh^2(kd)}{8\sinh^4(kd)}$$

$$F_1 = \tanh^5(kd)$$

$$F_2 = [kd/\sinh(kd)]^4 \tag{16}$$

Incorporating Eq. (15) into the parabolic model based on Eq. (13) leads to:

$$\begin{aligned} &c_g A_x + i(\bar{k} - a_0 k)c_g A + \frac{1}{2}(c_g)_x A \\ &\quad + \frac{i}{\omega}\left(a_1 - b_1\frac{\bar{k}}{k}\right)(cc_g A_y)_y - \frac{b_1}{\omega k}(cc_g A_y)_{yx} \\ &\quad + \frac{b_1}{\omega}\left(\frac{k_x}{k^2} + \frac{(c_g)_x}{2kc_g}\right)(cc_g A_y)_y \\ &\quad + \frac{i\omega}{2}\left[(1+DF_1(ka)^2)\frac{\tanh(kd + F_2 ka)}{\tanh(kd)} - 1\right]A \\ &\quad = 0 \end{aligned} \tag{17}$$

where the subscripts represent derivatives.

Saied and Tsanis (2004) developed a set of generalized Padé approximations for the square root in Eq. (8) centred at a certain wave angle $\theta=\theta_b$. The error in calculating l with this method is effectively zero at $\theta=\theta_b$. The model based on the generalized [1/1] Padé approximation has the same form as Eq. (17). However, the coefficients a_0, a_1, and b_1 in Eq. (13) can be given as functions of the wave angles as follows:

$$a_0 = \frac{\cos\theta_b(4 - \sin^2\theta_b)}{4 - 3\sin^2\theta_b}$$

$$a_1 = \frac{-3\cos\theta_b}{4 - 3\sin^2\theta_b}$$

$$b_1 = \frac{-1}{4 - 3\sin^2\theta_b} \tag{18}$$

Saied and Tsanis (2004) showed that for θ_b=55°, the error in calculating l does not exceed 5% for

wave angles up to 70°. Therefore, a rational approximation based on Eqs. (13) and (18) with θ_b=55° can be comparable to the [2/2] Padé approximation or the minimax approximation. However, the main advantage of Eq. (18) over the minimax approximation is that it is more accurate whenever the wave angle θ is known or can be approximately estimated. The higher-order model of Kirby (1986a) based on [1/1] conventional Padé approximation is a special case from Eq. (18) where the coefficients a_0, b_0 and b_1 can be obtained by setting θ_b=0°.

A new parabolic model is developed based on Eqs. (17) and (18) in which a marching scheme is implemented based on Crank–Nicolson scheme (given by Kirby, 1986b). The angle θ_b is estimated from the previously calculated upstream grid points as follows:

$$m = Im\left(\frac{\partial A/\partial y}{kA}\right)$$

$$l = \left[Im\left(\frac{\partial A/\partial y}{A}\right) + \bar{k}\right]\Big/ k$$

$$\theta_b = \tan^{-1}(m/l) \tag{19}$$

The angle θ_b is required at $i-(1/2)$, where i is the index of the line at which the wave potential is calculated along the longshore direction from j=1 to $j=j_{max}$. However, for the first iteration, the angle θ_b is calculated at $i-(3/2)$. Generally, the wave angle is calculated between two lines $i1$ and $i2$ and at the row j from Eq. (19) as follows:

$$m_{i1} = Im\left[\frac{A_{(i1,j+1)}-A_{(i1,j)}}{A_{(i1,j+1)}+A_{(i1,j)}} + \frac{A_{(i1,j)}-A_{(i1,j-1)}}{A_{(i1,j)}+A_{(i1,j-1)}}\right]\Big/(k\Delta y)$$

$$m_{i2} = Im\left[\frac{A_{(i2,j+1)}-A_{(i2,j)}}{A_{(i2,j+1)}+A_{(i2,j)}} + \frac{A_{(i2,j)}-A_{(i2,j-1)}}{A_{(i2,j)}+A_{(i2,j-1)}}\right]\Big/(k\Delta y)$$

$$m = (m_{i1} + m_{i2})/2$$

$$l = 2Im\left[\frac{A_{(i2,j)} - A_{(i2-1)}}{A_{(i2,j)} + A_{(i2-1,j)}}\right]\Big/(k\Delta x) + \frac{\bar{k}_{(i2,j)} + \bar{k}_{(i2-1,j)}}{2}$$

$$\theta_b = \tan^{-1}(m/l) \tag{20}$$

where i index increases in direction of wave starting from 1 at the offshore boundary and j index represents the alongshore direction.

Kirby (1986b) showed that results of the high-order model based on [1/1] conventional Padé approximation might be affected by the wave amplitude modulations that originate in areas of large bottom variations where the mild slope approximation is violated. These noisy unrealistic amplitude modulations can spread quickly to fill the lateral extent of the model grid. The calculation of wave angles using Eqs. (19) and (20) may be affected significantly by these short crested wave amplitude modulations. Kirby (1986b) showed that the most suitable approach to suppress the unrealistic noise is to filter the complex wave potential based on:

$$A_j^* = cA_{j+1} + (1-2c)A_j + cA_{j+1} \tag{21}$$

where A_j^* is the filtered complex wave potential and c is a constant in the range $0.1<c<0.3$. This approach, however, can cause damping in the wave amplitudes. Therefore, for cases of large bottom variations, the wave angles are calculated using the filtered complex potential A_j^*, while the wave amplitudes and matrix coefficients are calculated using the unfiltered complex potential A_j. This method smoothes the wave angles, while keeps the wave amplitudes unchanged.

The lateral boundary conditions can either be an absorbing or generating boundary. A perfectly absorbing boundary condition is given by (Kirby, 1986c):

$$\frac{\partial A}{\partial y} = iAk\sin\theta \tag{22}$$

where θ is the wave angle at the boundary measured counterclockwise from the x-axis. Similarly, the generating boundary condition is given by:

$$\frac{\partial A}{\partial y} = ik\sin\theta\left(2A_g - A\right) \tag{23}$$

where A_g is the generating wave potential at the boundary. Estimation of wave angle θ at the boundary is based on Eq. (19) using the most recent upstream wave potential (Kirby, 1986c).

3. Model application and analysis

In order to test the new parabolic model for cases of complex bathymetry, the case reported by Berkhoff (1982) is considered. The experimental bathymetry consists of an elliptic shoal situating on a plane sloping beach of 1:50 slope. Fig. 1 shows the bottom contours of the computational domain along with the labelled transects 1–8 for which experimental data are available. The incident wave height is 0.0464 m and the wave period is 1 s. For a computational domain of 25×20 m, the grid size is $\Delta x=\Delta y=0.25$ m, which corresponds to 101×81 grid points. Three iterations for each column are required for convergence of Eq. (17). Fig. 2 shows the wave height pattern behind the elliptic shoal using the new parabolic model.

Comparison between the numerical results from the proposed generalized parabolic model and the experimental data along the eight transects as well as the results from the higher-order parabolic model of Kirby (1986a) are shown in Fig. 3a–h. Because the wave angles for this case are very small, the results of the two models are very close to each other as shown in Fig. 3. Kirby's (1986a) model results, however, seem to be closer to the experimental data for transect 6. The slight difference between the two models results may be explained by error in calculation of the wave angles by the proposed model through Eq. (19). Generally, it is concluded that the proposed model can simulate the wave pattern for complicated bathymetry very well.

In order to test the capability of the new parabolic model for wide wave angles, the circular shoal problem used to test the nonlinear parabolic model, which was developed by Li (1997), is adopted. Owing to the axisymmetry of the circular shoal, the wave focusing pattern behind the shoal should be independent of the incident wave angle if the model is correct (Dalrymple et al., 1989).

The water depth used is the same adopted by Dalrymple et al. (1989), which is:

$$h=\begin{cases} h_0 & r>R \\ h_0+\alpha-\beta\left[1-(0.2X')^2-(0.2Y')^2\right]^{1/2} & r<R \end{cases} \tag{24}$$

where h_0=0.336 m, α=0.12 and 0.18, β=0.2 and 0.3, R=4 m is the radius of the shoal, $r=(X'^2+Y'^2)^{1/2}$ and (X',Y')=coordinates with the origin at the crest of the shoal. The wave period is 1 s.

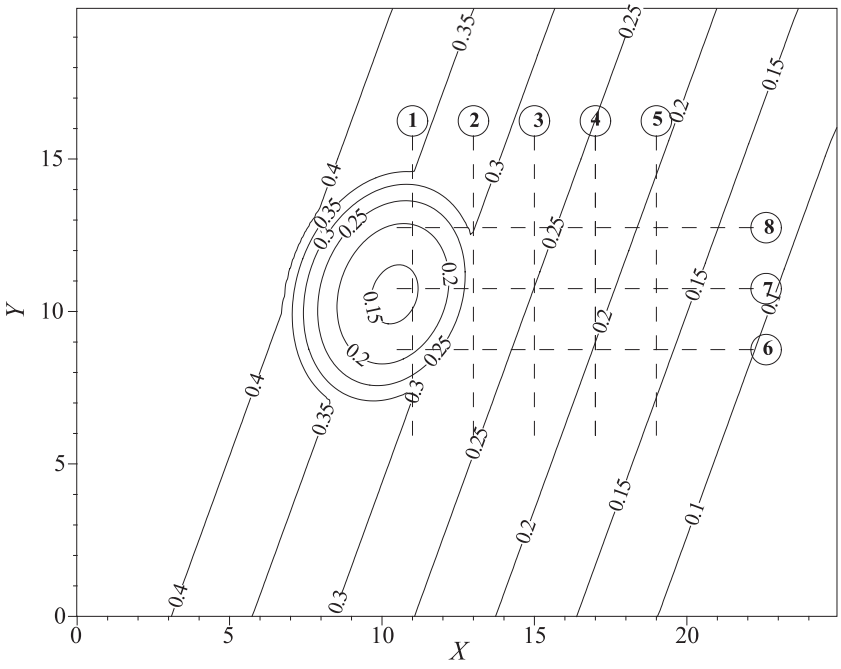

Fig. 1. Elliptic shoal bathymetry.

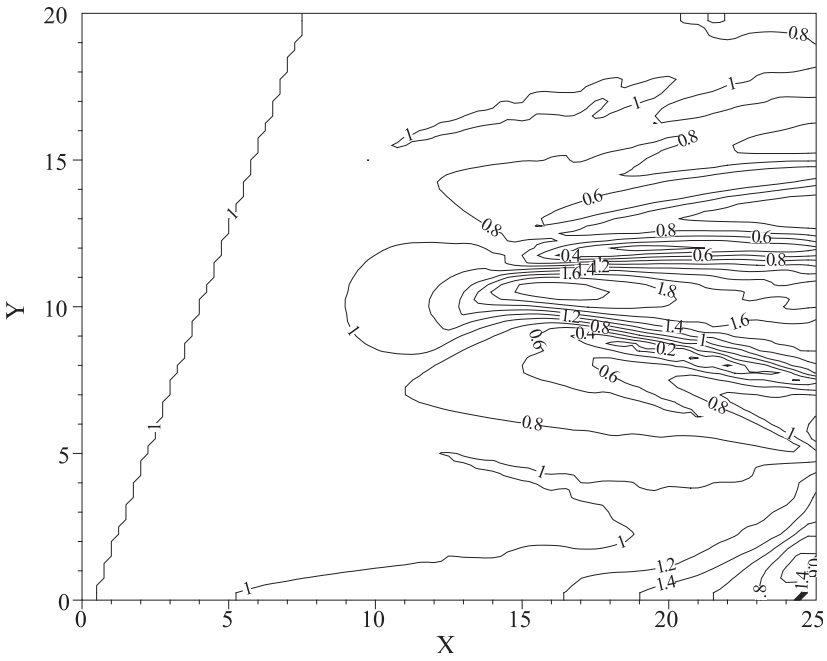

Fig. 2. Wave height pattern behind the elliptic shoal (new parabolic model).

Fig. 4 shows the wave height patterns behind the circular shoal using the new parabolic model for different incident wave angles. In Fig. 4a–c, the parameters α and β are chosen as 0.12 and 0.2, respectively. Fig. 4b and c, which correspond to wave angles 45° and 70°, respectively, are compared with Fig. 4a, which corresponds to the case of normal wave incidence. It can be shown that the overall agreement between the two cases and the case of normal incidence is good. The wave heights along the wave focusing crest are correct without any angle distortion. The symmetry, however, is distorted for the case of θ_0=70°.

In order to increase the shoal height and consequently the bottom variation, the values of 0.18 and 0.3 were assigned to the parameters α and β, respectively. The model results are filtered according to Eq. (21) using c=0.05 for the case of θ_0=70°. For the case of θ_0=45° (Fig. 4e), the wave heights along the wave focusing crest are correct without any angle distortion. The case of θ_0=70° (Fig. 4f), however, reports significant change of the wave heights along the wave focusing crest from the case of normal incidence but still without angle distortion. The symmetry is distorted for both cases especially for the case of θ_0=70°.

In order to compare Kirby's (1986b) model with the present model for wide wave angles, the same cases described above are resolved using Kirby's (1986b) model. Fig. 5 shows the results of Kirby's model. For θ_0=45°, the coefficients a_0, a_1 and b_1 in Eq. (13) are set to 0.999465861, −0.822482968 and −0.335107575, respectively, which corresponds to range of applicability up to 50°. For θ_0=70°, the range of applicability has to be increased to 80°, which corresponds to values of 0.985273164, −0.925464479 and −0.550974375 for the coefficients a_0, a_1 and b_1, respectively. Fig. 5 shows very similar results to the present model in cases of θ_0=45° (Fig. 5a and c). For the case of wide wave angle (θ_0=70°), significant shift towards the downstream of the wave pattern behind the shoal is evident in (Fig. 5b and d). Due to the error in the wave angle calculation through Eq. (19), the proposed model's results for the case of θ_0=70° and large bottom variations seem to be noisier than the results of Kirby's (1986b) model as shown in Fig. 4f and d, respectively. However, due to the downstream shift

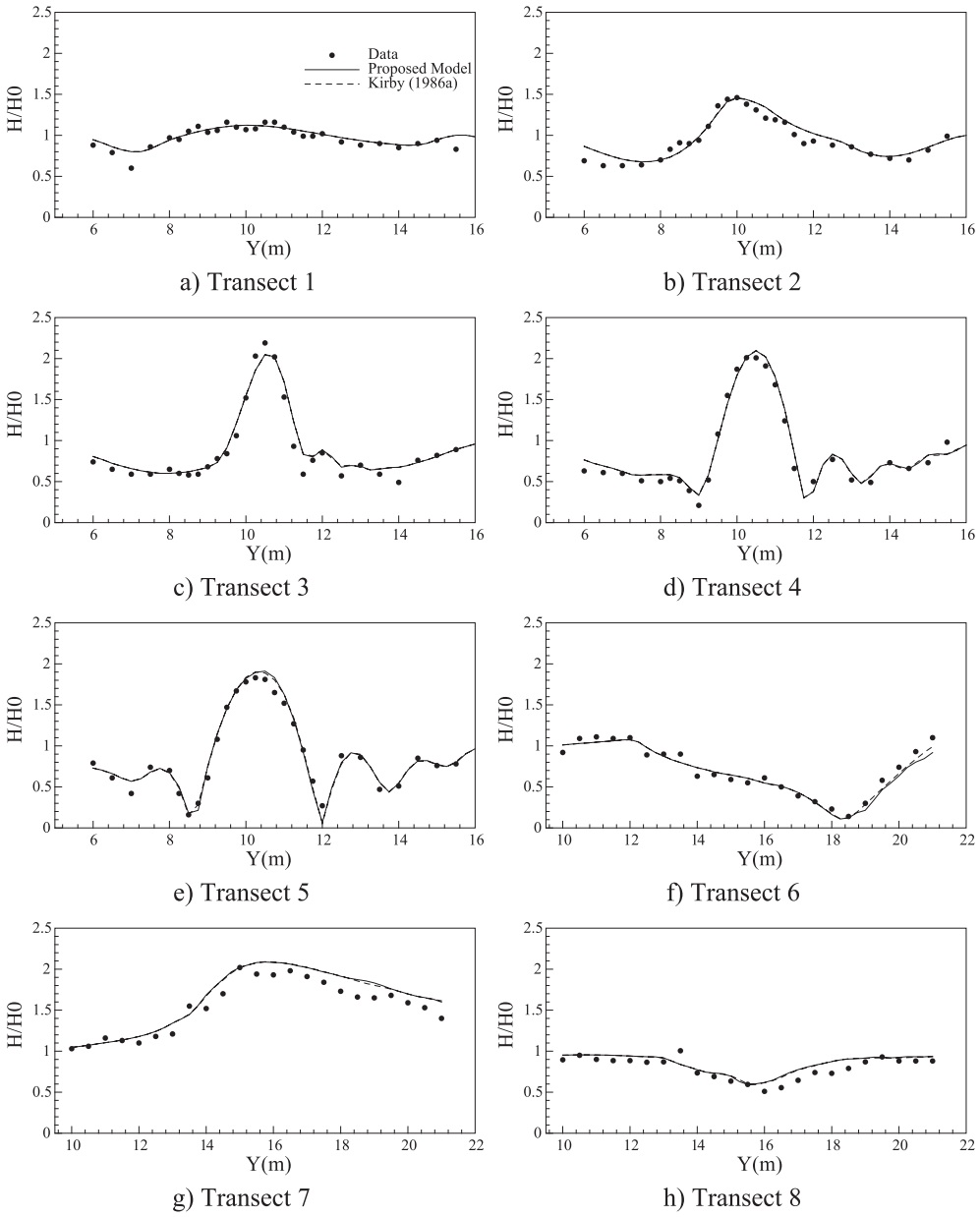

Fig. 3. Comparison between experimental and computational results for the elliptic shoal case.

of the wave focusing pattern in Kirby's (1986b) model results, the proposed model results are closer to the case of normal wave incidence (Fig. 4d).

Fig. 6a–b shows the longitudinal sections along the wave focusing crests for the current model and Kirby's (1986b) model. It can be shown that both models perform well for the two cases of θ_0=45°. However, the present model is better as Kirby's (1986b) model underestimates the wave heights behind the shoal crest.

For the cases of θ_0=70°, Kirby's (1986b) model significantly underestimates the wave heights behind the shoal due to the shift in the wave focusing pattern, which confirms that the present model

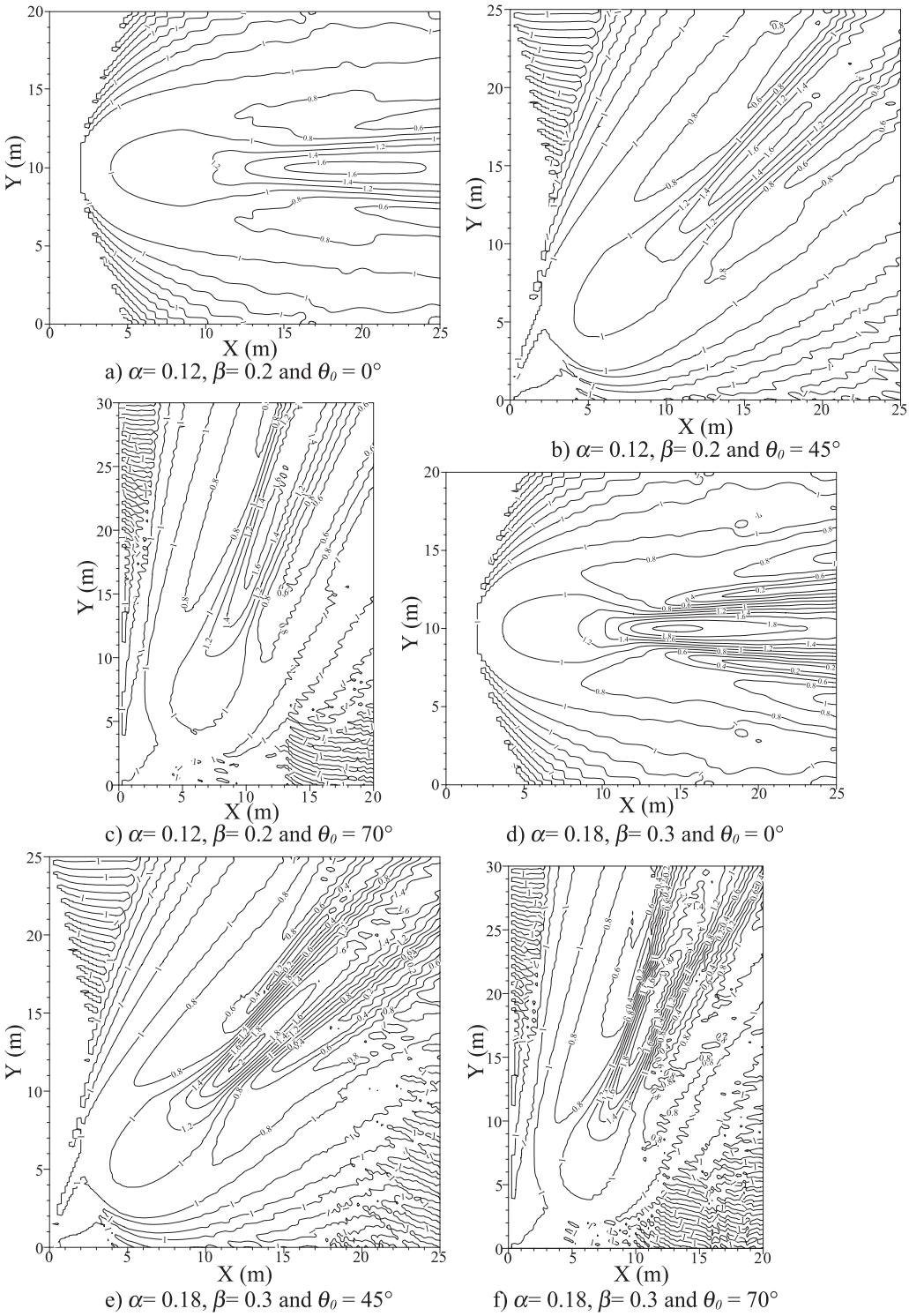

Fig. 4. Wave height patterns behind the circular shoal using the new parabolic model.

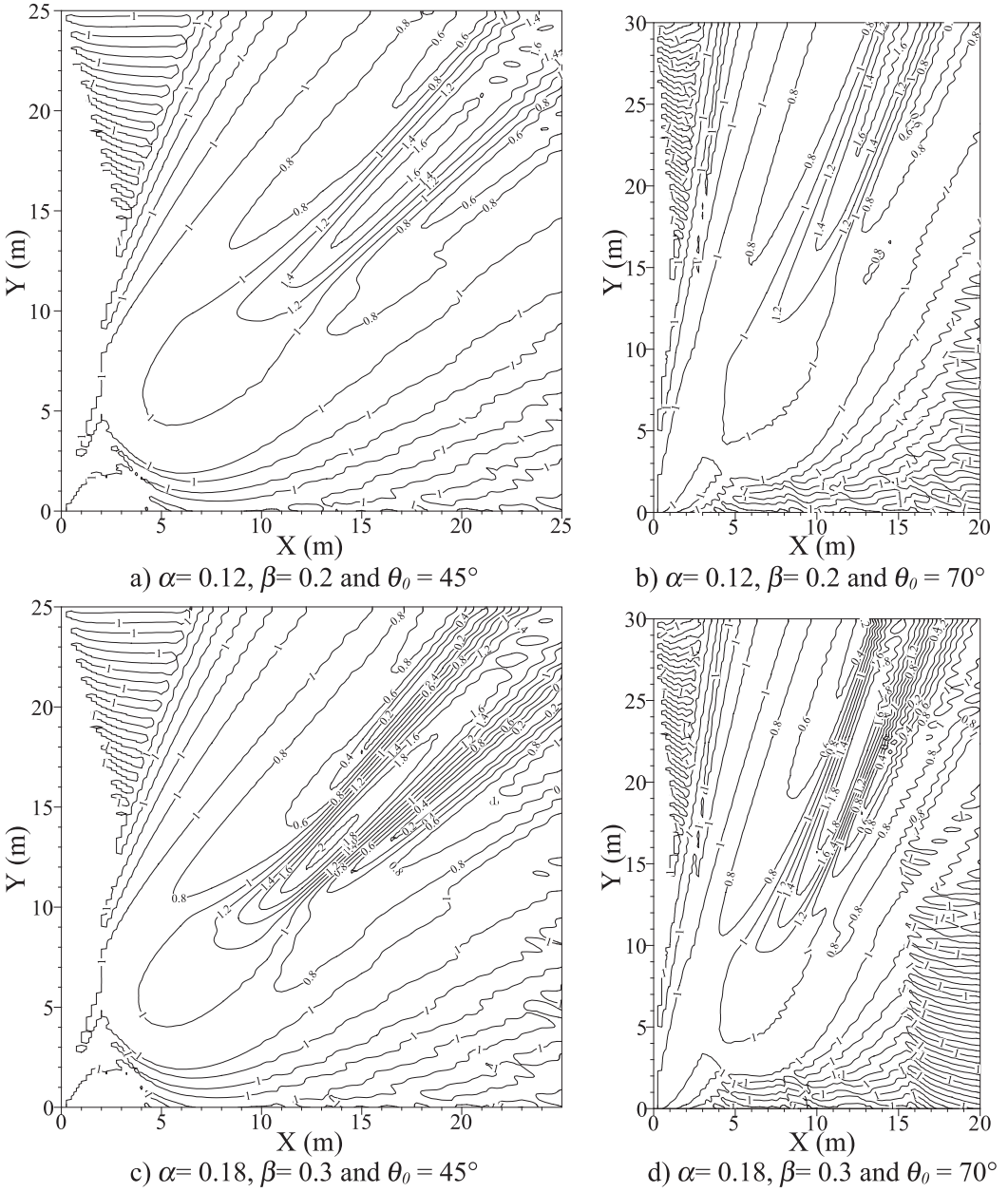

Fig. 5. Wave height patterns behind the circular shoal using Kirby's (1986b) model with angle ranges 50° (for a and c) and 80° (for b and d).

performs better for wide angles as well. For the case of large bottom variation and large incident wave angle (θ_0=70°), the noisy results of the present model are evident as shown in Fig. 6b, which affects the calculation of wave angles and consequently the model results.

The results of Li's (1997) model for the same cases were inspected as well. Due to the upwind scheme used in his model, Li (1997) reported that Kirby's (1986b) is better for small wave angles, which implicitly implies that the present model is better as well because it is better than Kirby's

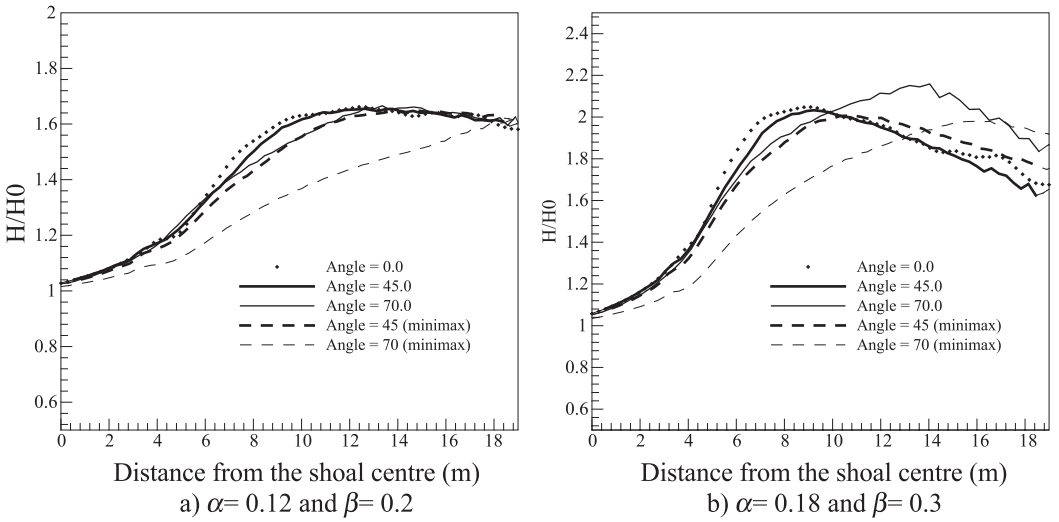

Fig. 6. Longitudinal sections along the centre of the shoal (in the direction of wave propagation).

(1986b). For the case of θ_0=70° and small bottom variations (i.e. α=0.12 and β=0.2), Li (1997) reported slight shift of the wave pattern behind the shoal crest. Being less than the shift reported by Kirby's (1986b) model, Li's (1997) model is the better for this case. The present model, however, is more accurate for this case as shown in Figs. 4c and 6a. For the large bottom variation case (i.e. α=0.18 and β=0.3) with θ_0=70°, after inspecting Li's (1997) model results, it can be shown that in addition to the shift of the wave pattern towards the downstream, the wave pattern immediately behind the shoal crest is shifted in the x-direction (the direction at which the line by line solution is performed). This may be explained by the upwind scheme implemented in this model. However, Li's (1997) model results for this particular case are smoother than the results of the present model due to the effect of the noisy results of the present model in calculating the wave angles.

Table 1
Favourable parabolic model for respective wave angle and bottom variation combinations

	Small wave angles (≤45°)	Large wave angles (>45°)
Small bottom variations	Present model	Present model
Large bottom variations	Present model	Li's (1997) model

Based on the preceding discussion, Table 1 illustrates the favourable parabolic model for respective wave angle and bottom variation combinations.

4. Conclusions

The parabolic model based on the generalized [1/1] Padé approximation for the elliptic mild slope equation performs better than all the existing parabolic models based on rational approximation for large wave angles. The model can simulate wave patterns for complicated bathymetry. The numerical test case of the circular shoal confirms that the new parabolic model can simulate the wave pattern behind the shoal for very large angles up to 70°. Comparison between the new model, Kirby's (1986b) model and Li's (1997) model results shows that the new model can simulate the wave heights behind the circular shoal better than the other two models. Li's (1997) model performance for cases of very wide wave angles with large bottom variations is smoother than the current model due to the error in wave angle calculation by the new model. The new model is more user friendly than Kirby's (1986b) model because the coefficients a_0, a_1 and b_1 are calculated internally unlike Kirby's (1986b) model where the user has to specify a certain range of applicability for wave angles.

References

Berkhoff, J.C.W., 1972. Computation of combined refraction–diffraction. Proc. 13th Coastal Eng. Conf., vol. 1. ASCE, Vancouver, pp. 471–490.

Berkhoff, J.C.W., 1982. Refraction and diffraction of water waves; wave deformation by a shoal, comparison between computations and measurements, report on mathematical investigation, Delft Hydraulics Laboratory, Report W 154 part VIII.

Booij, N., 1981. Gravity waves on water with non-uniform depth and current. Report No. 81-1, Delft University of Technology, Dept. of Civil Eng.

Dalrymple, R.A., Kirby, J.T., 1988. Models for very wide-angle water waves and wave diffraction. J. Fluid Mech. 192, 33–50 (Cambridge, UK).

Dalrymple, R.A., Suh, K.D., Kirby, J.T., Chae, J.W., 1989. Models for very wide-angle water waves and wave diffraction: 2. Irregular bathymetry. J. Fluid Mech. 201, 299–322 (Cambridge, UK).

Kirby, J.T., 1986a. Higher-order approximations in the parabolic equation method for water waves. J. Geophys. Res. 91 (C1), 933–952.

Kirby, J.T., 1986b. Rational approximations in the parabolic equation method for water waves. Coast. Eng. 10, 355–378.

Kirby, J.T., 1986c. Open boundary condition in parabolic equation method. J. Waterw. Port Coast. Ocean Eng. 112 (3), 460–465.

Kirby, J.T., Dalrymple, R.A., 1986. An approximate model for nonlinear dispersion in monochromatic wave propagation models. Coast. Eng. 9, 545–561.

Li, B., 1997. Parabolic model for water waves. J. Waterw. Port Coast. Ocean Eng. 123 (4), 192–199.

Radder, A.C., 1979. On the parabolic equation method for water wave propagation. J. Fluid Mech. 91 (1), 159–176 (Cambridge, UK).

Saied, U.M., Tsanis, I.K., 2004. Improved boundary equations for elliptic water wave models. Coast. Eng. 51 (1), 17–34.